

Intro

# Light Propagation in Free Space

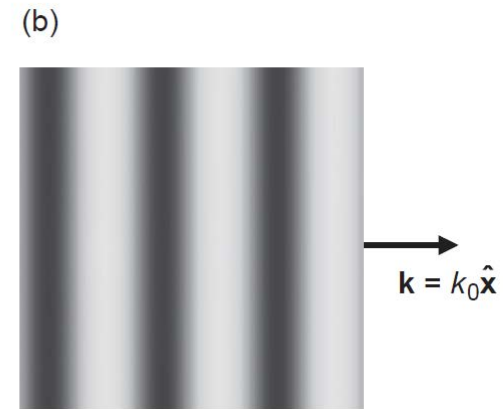
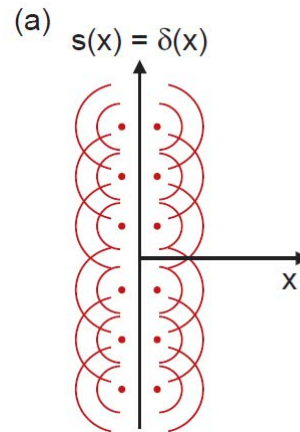
- Helmholtz Equation

$$\nabla^2 U(\mathbf{r}, \omega) + k_0^2 U(\mathbf{r}, \omega) = s(\mathbf{r})$$

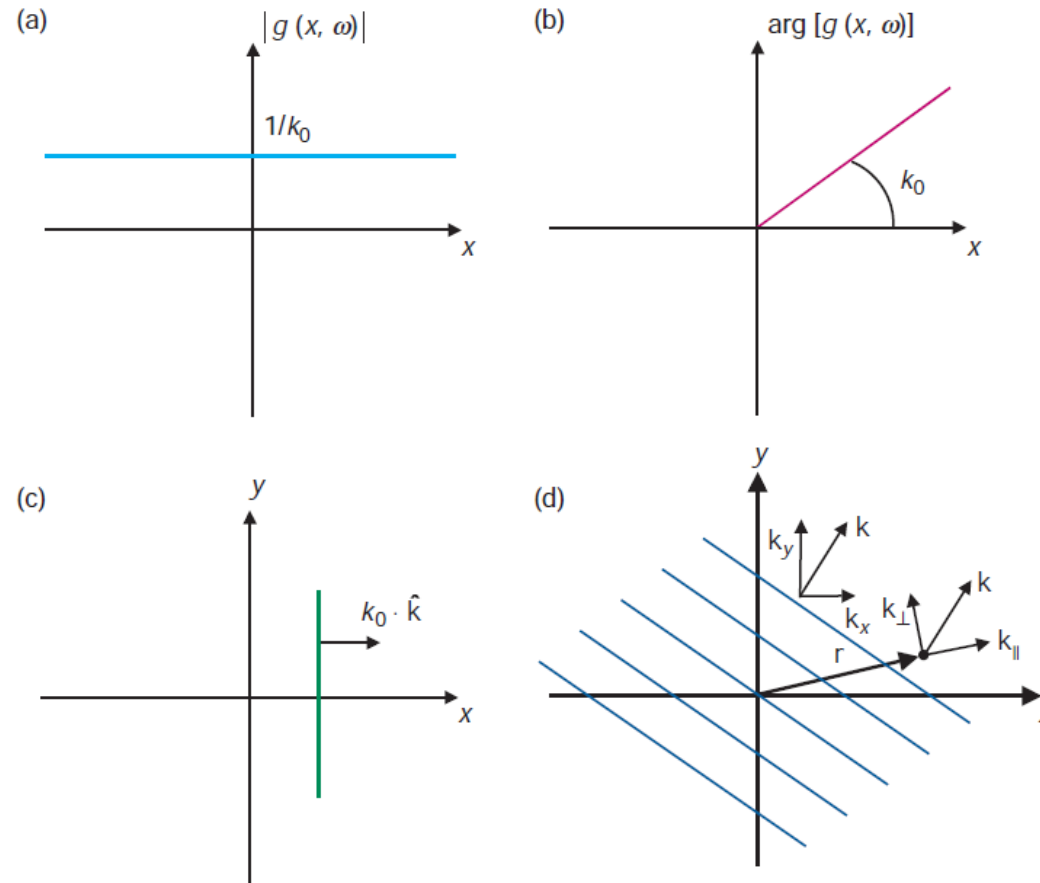
- 1-D Propagation

- Plane waves  $\frac{\partial^2 g(x, \omega)}{\partial x^2} + k_0^2 g(x, \omega) = \delta(x)$

$$g(\mathbf{r}, \omega) = \frac{i}{2k_0} e^{ik_0 \cdot \hat{\mathbf{k}} \cdot \mathbf{r}}$$



# Plane wave propagation



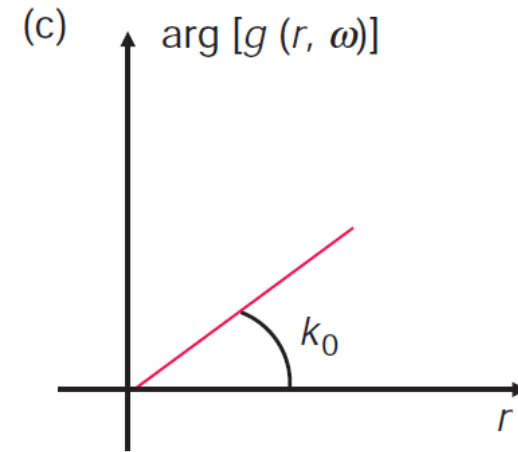
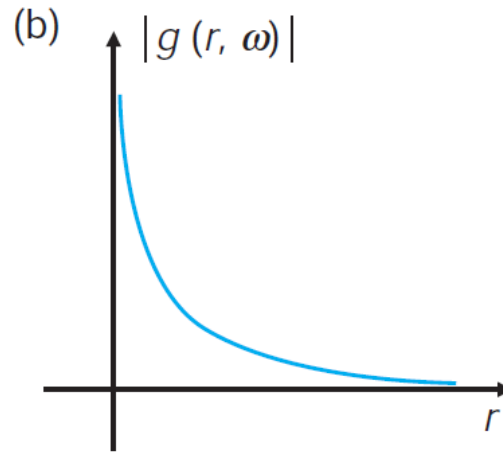
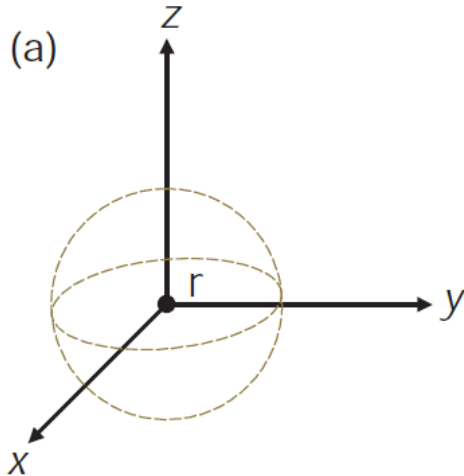
# Light Propagation in Free Space

- 3-D Propagation

$$\nabla^2 g(\mathbf{r}, \omega) + k_0^2 g(\mathbf{r}, \omega) = \delta^{(3)}(\mathbf{r})$$

- Spherical Waves

$$g(\mathbf{r}, \omega) = \frac{e^{ik_0 r}}{r}$$



# Huygen's Principle

- Each point reached by the field becomes a secondary source, which emits a new spherical wavelet and so on.

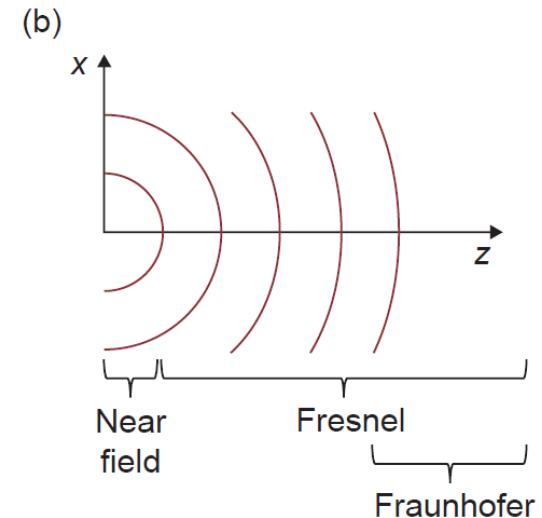
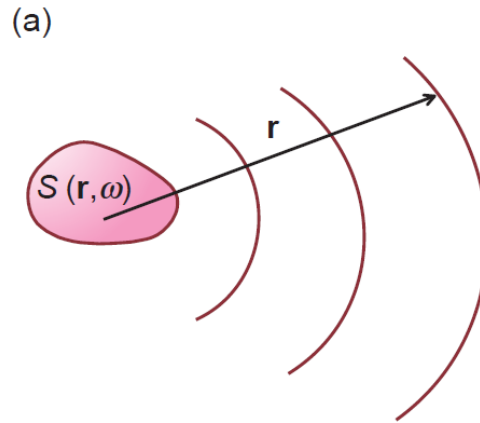
$$U(\mathbf{r}, \omega) = \int_V s(\mathbf{r}', \omega) \cdot \frac{e^{ik_0|\mathbf{r}-\mathbf{r}'|}}{|\mathbf{r}-\mathbf{r}'|} d^3\mathbf{r}'$$

- Generally this integral is hard to evaluate

# Fresnel Approximation of Wave Propagation

- The spherical wavelet at far field is now approximated by

$$g(\mathbf{r}, \omega) \simeq \frac{e^{ik_0 z}}{z} \cdot e^{ik_0 \frac{x^2 + y^2}{2z}}$$



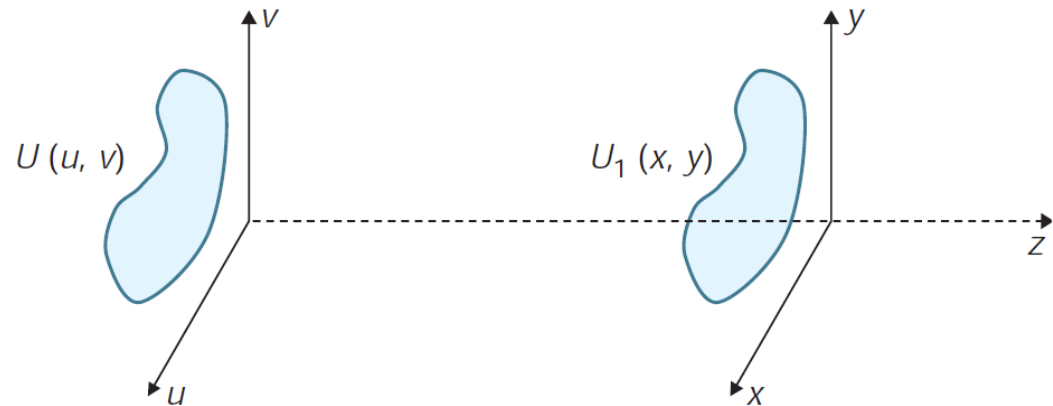
# Fresnel Approximation of Wave Propagation

- For a given planar field distribution at  $z = 0$ ,  $U(u, v)$ , we can calculate the resulting propagated field at distance  $z$ ,  $U(x, y, z)$  by convolving with the Fresnel wavelet  

$$e^{ik_0[(x^2+y^2)/2z]}$$

$$U_1(x, y, z) = \frac{e^{ik_0z}}{z} \cdot \int_{-\infty}^{\infty} \int_{-\infty}^{\infty} U(u, v) \cdot e^{\frac{ik_0}{2z}[(x-u)^2+(y-v)^2]} du dv$$

$$\propto U \circledast e^{ik_0\left(\frac{x^2+y^2}{2z}\right)}$$



# Fourier Transform Properties of Free Space

- **Fraunhofer approximation** is valid when the observation plane is even farther away. And the quadratic phase becomes

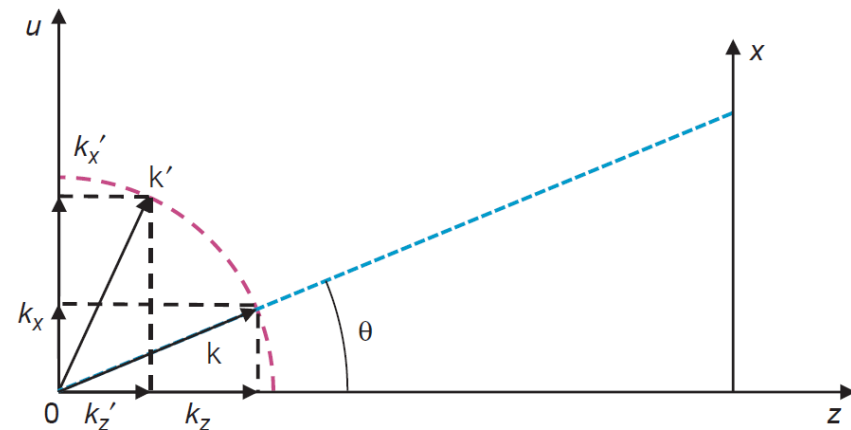
$$\frac{ik_0}{2z}[(x-u)^2 + (y-u)^2] \simeq \frac{ik_0}{2z}(-2xu - 2yv)$$

- The field distribution then is described as a Fourier transform

$$U_1(k_x, k_y) = \int_{-\infty}^{\infty} \int_{-\infty}^{\infty} U(u, v) \cdot e^{-i(k_x u + k_y v)} du dv$$

$$k_x = \frac{k_0 x}{z} = \frac{2\pi x}{\lambda z}$$

$$k_y = \frac{k_0 y}{z} = \frac{2\pi y}{\lambda z}$$





# Fourier Transform Properties of Lenses

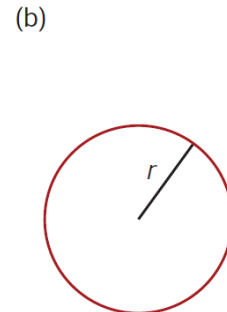
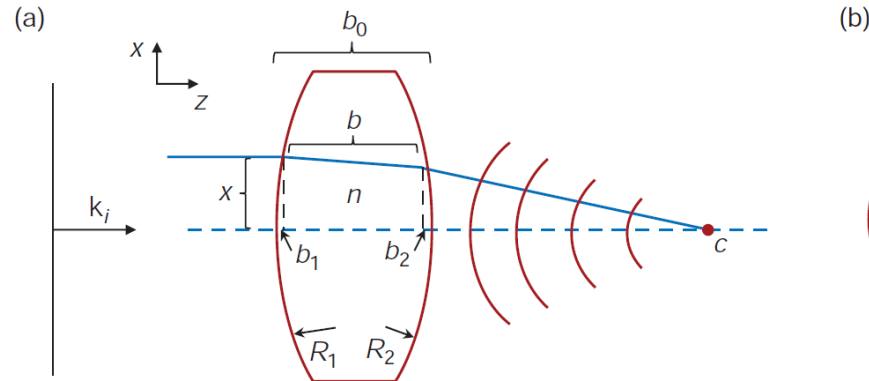
- Lenses have the capability to perform Fourier Transforms, eliminating the need for large distances of propagation.
- Transmission function in the form of

$$t(x, y) = e^{i\phi(x, y)}$$

$$\phi(r) = \phi_0 - \frac{k_0 r^2}{2} (n - 1) \left( \frac{1}{R_1} - \frac{1}{R_2} \right) \quad \text{where } \phi_0 = k_0 \cdot b_0$$

$$\phi(r) = \phi_0 - \frac{k_0 r^2}{2f}$$

$$\frac{1}{f} = (n - 1) \left( \frac{1}{R_1} - \frac{1}{R_2} \right)$$

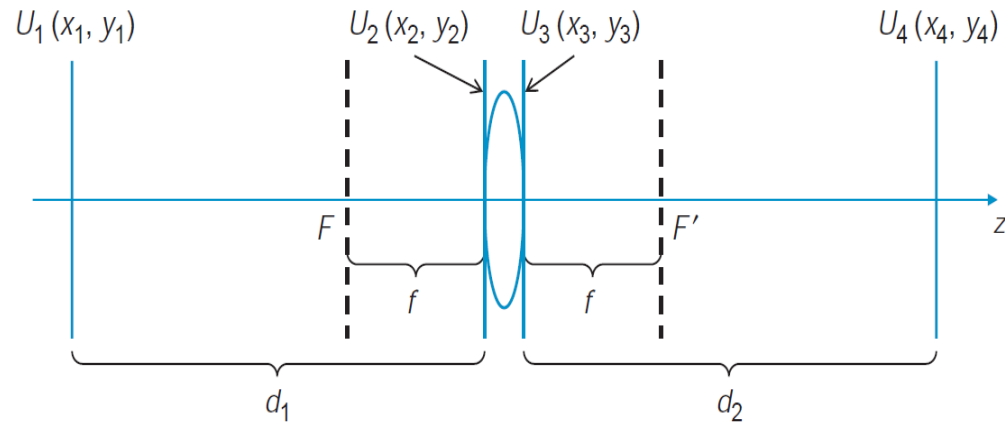


# Fourier Transform Properties of Lenses

$$U_2(x_2, y_2) = U_1(x_1, y_1) \odot e^{i \frac{k_0(x_1^2 + y_1^2)}{2d_1}}$$

$$U_3(x_3, y_3) = U_2(x_2, y_2) \cdot e^{-i \frac{k_0(x_2^2 + y_2^2)}{2f}}$$

$$U_4(x_4, y_4) = U_3(x_3, y_3) \odot e^{i \frac{k_0(x_3^2 + y_3^2)}{2d_2}}$$



$$U_4(k_{x4}, k_{y4}) = \int_{-\infty}^{\infty} \int_{-\infty}^{\infty} U_1(x_1, y_1) \cdot e^{-i(k_{x4} \cdot x_1 + k_{y4} \cdot y_1)} dx_1 dy_1$$

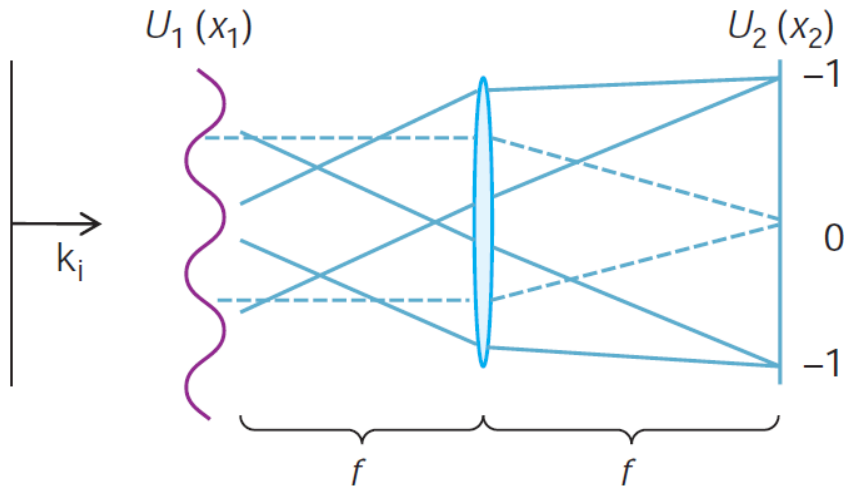
$$k_{x4} = \frac{2\pi x_4}{\lambda f}$$

$$k_{y4} = \frac{2\pi y_4}{\lambda f}$$

# Fourier Transform Properties of Lenses

- Fourier transform of the field diffracted by a sinusoidal grating.

$$\begin{aligned}
 U(x_2) &= \int_{-\infty}^{\infty} \left[ 1 + \cos\left(\frac{2\pi x_1}{\Lambda}\right) \right] \cdot e^{-i\frac{2\pi x_1 x_2}{\lambda f}} dx_1 \\
 &= \frac{1}{2} \delta\left(\frac{2\pi x_2}{\lambda z} - \frac{2\pi}{\Lambda}\right) + \frac{1}{2} \delta\left(\frac{2\pi x_2}{\lambda z} + \frac{2\pi}{\Lambda}\right) + \delta(0)
 \end{aligned}$$



# Chap. 5

Light Microscopy

# Abbe's Theory of Imaging

- One way to describe an imaging system (e.g., a microscope) is in terms of a system of two lenses that perform two successive Fourier Transforms.

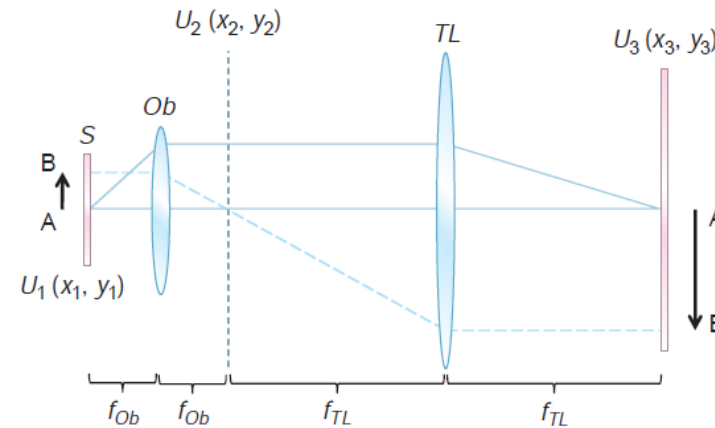
$$F\{F[f(x, y)]\} = f(-x, -y)$$

$$U_3(x_3, y_3) = U_1\left(-\frac{x_1}{M}, -\frac{y_1}{M}\right)$$

- Magnification is given by

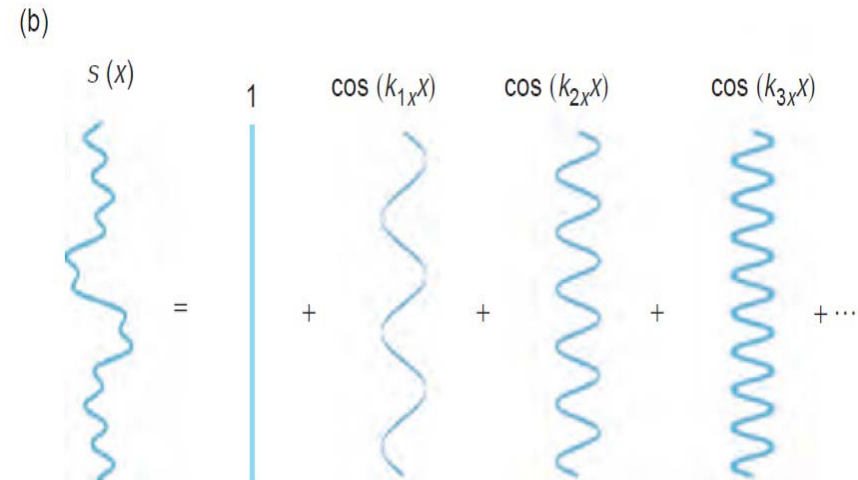
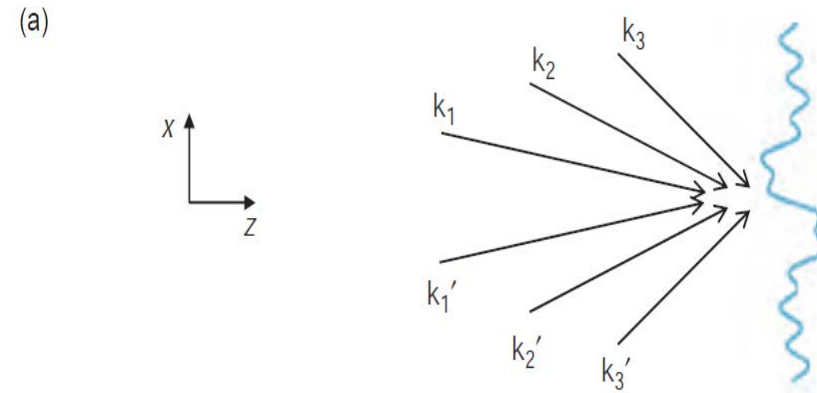
$$M = \frac{f_{TL}}{f_{Ob}}$$

- Cascading many imaging systems does not mean unlimited resolution!



# Resolution Limit

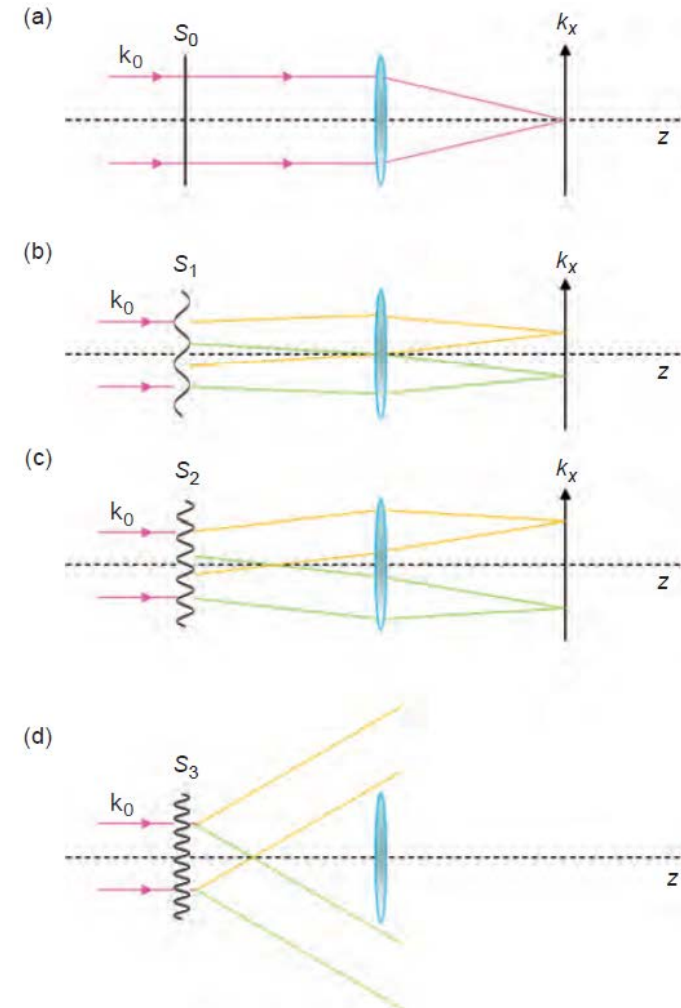
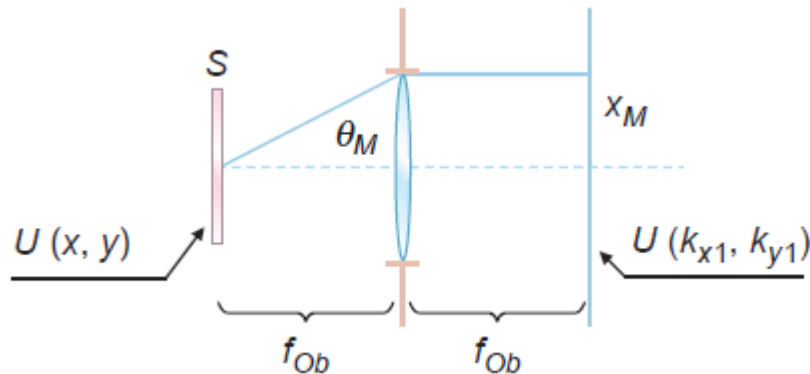
- “The microscope image is the interference effect of a diffraction phenomenon” – Abbe, 1873
- The image field can therefore be decomposed into sinusoids of various frequencies and phase shifts



# Resolution Limit

- the apertures present in the microscope objective limit the maximum angle associated with the light scattered by the specimen.
- The effect of the objective is that of a *low-pass filter*, with the cut-off frequency in 1D given by

$$k_M = \frac{2\pi}{\lambda f_{Ob}} \cdot x_M = \frac{2\pi}{\lambda} \cdot \theta_M$$



# Resolution Limit

- The image is truncated by the pupil function at the frequency domain

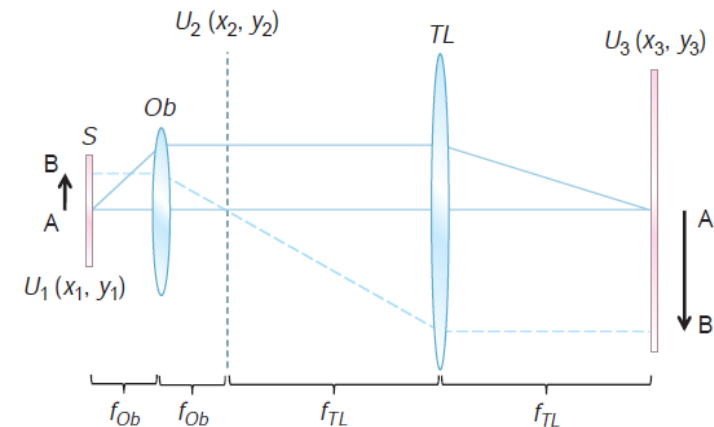
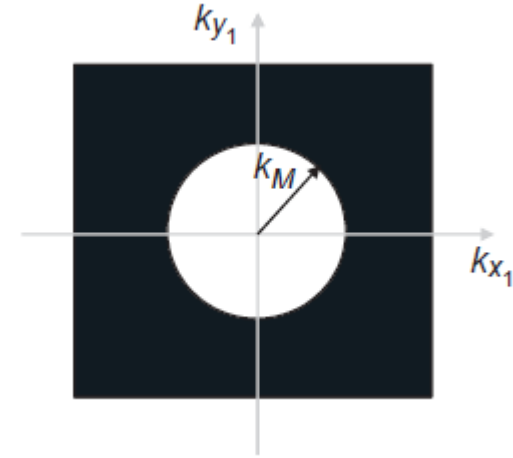
$$\underline{U}_2(k_{x2}, k_{y2}) = U_2(k_{x2}, k_{y2}) \cdot P(k_{x2}, k_{y2})$$

$$P(k_{x2}, k_{y2}) = \begin{cases} 1, & \text{if } k_{x2}^2 + k_{y2}^2 \leq k_M^2 \\ 0, & \text{otherwise} \end{cases}$$

$$= \Pi(k/2k_M)$$

- The resulting field is then the convolution of the original field and the Fourier Transform of P

$$\underline{U}_3(x_3, y_3) = U_1(x_3/M, y_3/M) \otimes g(x_3, y_3)$$





# Resolution Limit

- function  $g$  is the Green's function or PSF of the instrument, and is defined as

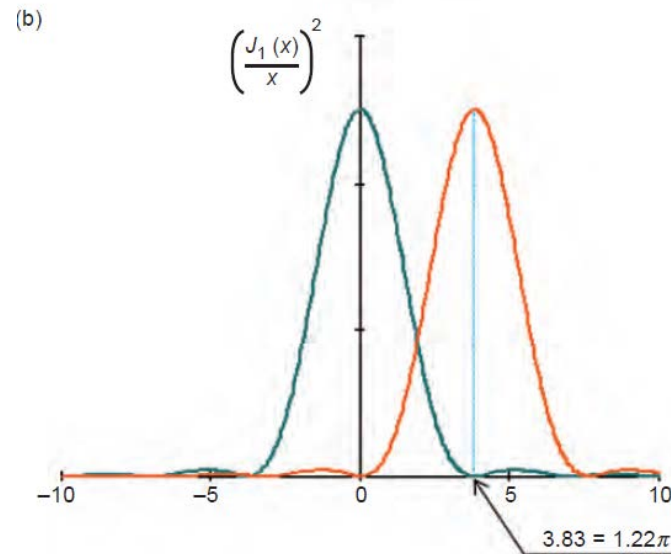
$$g(x_3, y_3) = \int_{-\infty}^{\infty} \int_{-\infty}^{\infty} P(k_{x2}, k_{y2}) \cdot e^{i(k_{x2} \cdot x_3 + k_{y2} \cdot y_3)} dk_{x2} dk_{y2}$$

- The Rayleigh criterion for resolution: maxima separated by at least the first root.

$$2\pi \frac{r_M}{\lambda f_{Ob}} \cdot \rho_0 = 1.22\pi$$

- Resolution:

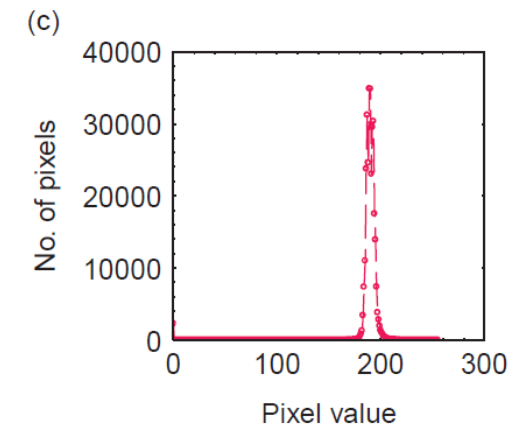
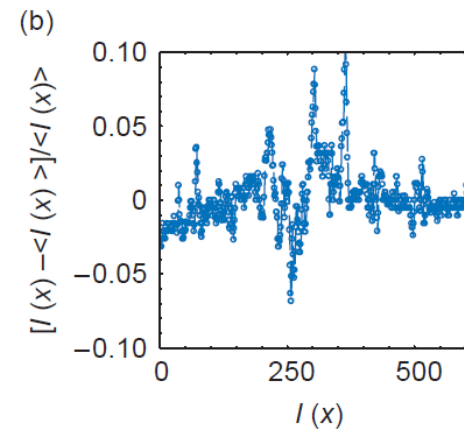
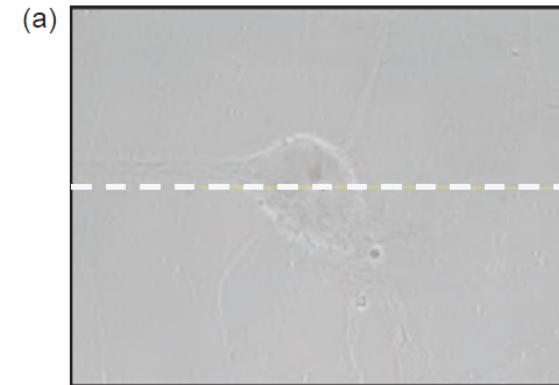
$$\rho_0 = 0.61 \frac{\lambda}{NA}$$



# Imaging of Phase Objects

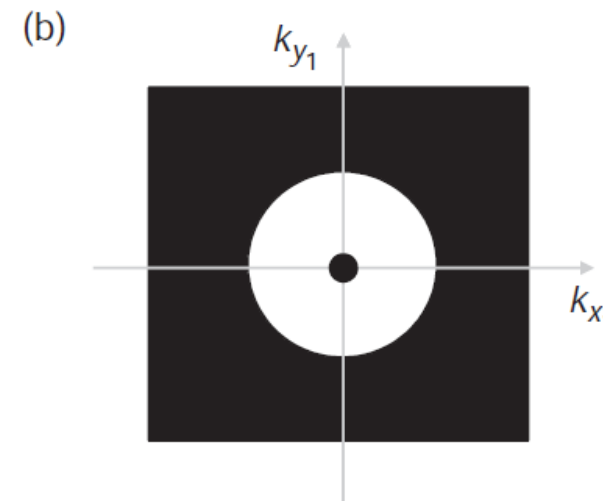
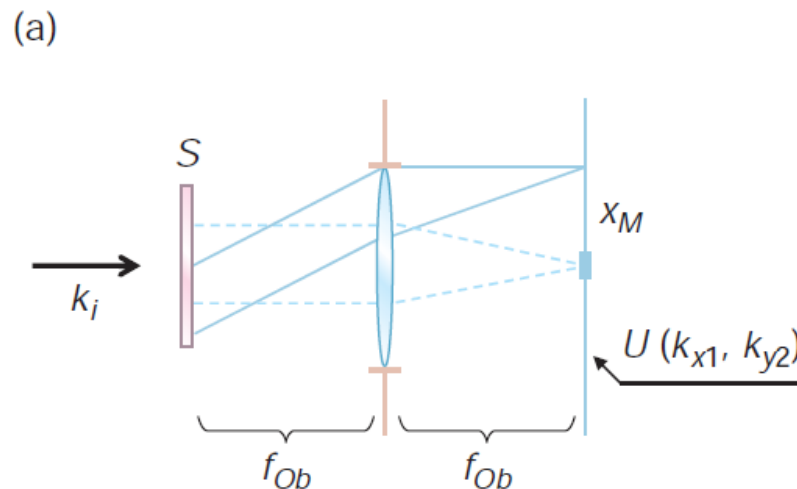
- Complex transmission function:  $A_s e^{i\phi_s(x,y)}$
- For transparent specimen,  $A_s$  is constant and so is  $A_i$  for an ideal imaging system.
- Detector at image plane are only sensitive to intensity, therefore zero contrast for imaging transparent specimen

$$I_i = |A_i \cdot e^{i\phi(x,y)}|^2 = A_i^2$$



# Dark Field Microscopy

- One straightforward way to increase contrast is to remove the low-frequency content of the image, i.e. DC component, before the light is detected.
- For coherent illumination, this high pass operation can be easily accomplished by placing an obstruct where the incident plane wave is focused on axis.



# Zernike's Phase Contrast Microscopy

- Developed in the 1930s by the Dutch physicist Frits Zernike
- Allows **label-free, noninvasive** *investigation* of live cells
- Interpreting the field as spatial average  $U_0$  and the fluctuating components,  $U_1(x, y)$

$$\begin{aligned}U(x, y) &= U_0 + [U(x, y) - U_0] \\ &= U_0 + U_1(x, y)\end{aligned}$$

- Note that the average  $U_0$  must be taken inside the coherence area. Phase is not well defined outside coherence area.

# Zernike's Phase Contrast Microscopy

- The field in Fourier Domain can be interpreted as the incident field and the scattered field.

$$\tilde{U}(k_x, k_y) = \delta(0, 0) + \tilde{U}_1(k_x, k_y)$$

- The image field is described as the interference between these two fields.

$$\begin{aligned} I(x, y) &= |U(x, y)|^2 \\ &= |U_0|^2 + |U_1(x, y)|^2 + 2|U_0| \cdot |U_1(x, y)| \cdot \cos[\Delta\phi(x, y)] \end{aligned}$$

- The key to PCM: the image intensity, unlike the phase, is very sensitive to  $\Delta\phi$  changes around  $\phi/2$ . The Taylor expansion around zero of cosine is negligible for small x, but linear dependent for sine

$$\begin{aligned} \cos(x) &\approx 1 - x^2/2, \\ \sin(x) &\approx x. \end{aligned}$$

# Zernike's Phase Contrast Microscopy

- By placing a small metal film that covers the DC part in the Fourier Plane can both attenuate and shift the phase of the unscattered field.

$$U^{PC}(x, y) = a \cdot e^{i\alpha} + U_1(x, y)$$

$$= a \cdot e^{i\alpha} + e^{i\phi(x, y)} - 1$$

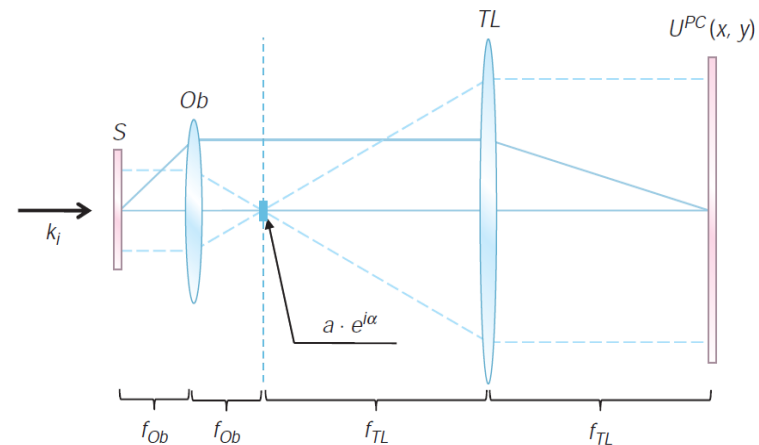
$$I^{PC}(x, y) = a^2 + 1 + 1 + 2[a \cos(\alpha + \phi) - a \cos \alpha - \cos \phi]$$

$$= a^2 + 2[1 - a \cos \alpha - \cos \phi + a \cos(\alpha + \phi)]$$

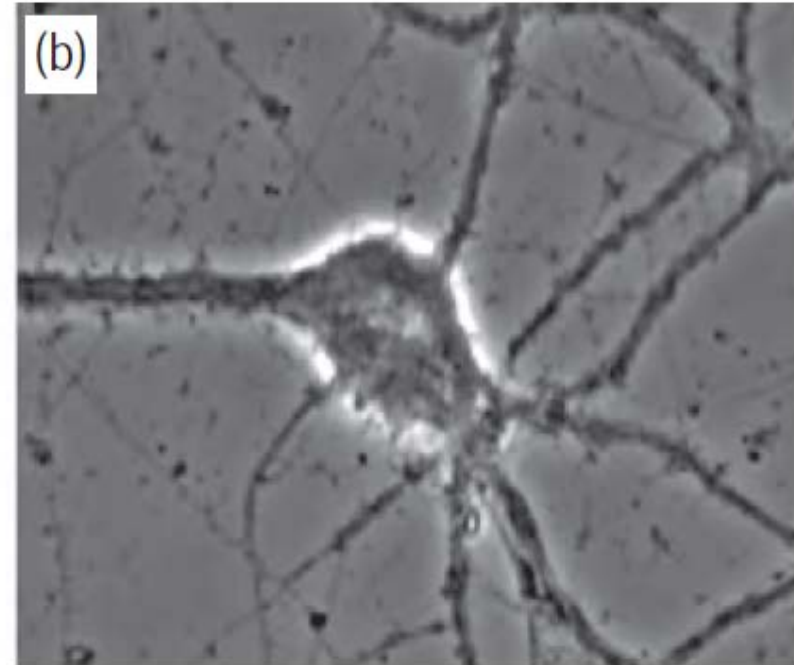
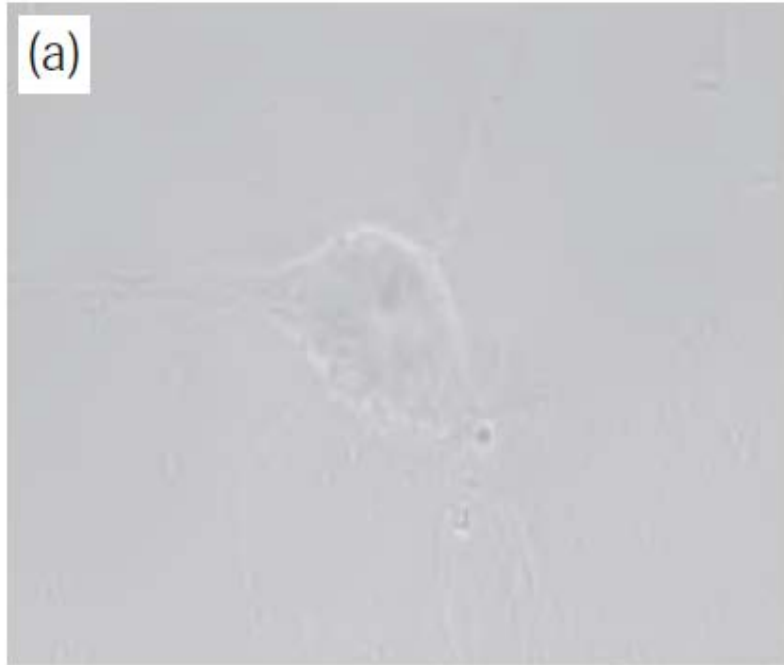
- If  $\phi = \frac{\pi}{2}$  is chosen.

$$I^{PC}(x, y) = a^2 \pm 2a \sin \phi(x, y)$$

$$\simeq a^2 \pm 2a\phi(x, y)$$



# Zernike's Phase Contrast Microscopy



# Chap. 6

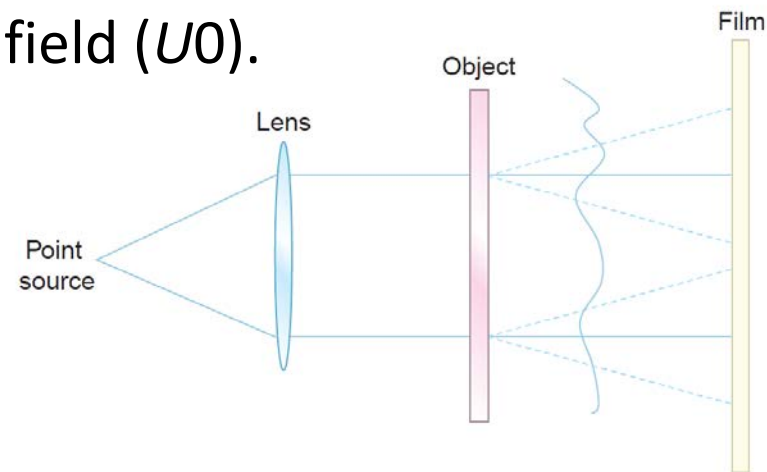
Holography



# Gabor's (In-Line) Holography

- In 1948, Dennis Gabor introduced “A new microscopic principle”,<sup>1</sup> which he termed holography (from Greek holos, meaning “whole” or “entire,” and grafe, “writing”).
- Record **amplitude** and **phase**
- Film records the Interference of light passing through a semitransparent object consists of the scattered ( $U_1$ ) and unscattered field ( $U_0$ ).

$$\begin{aligned} I(x, y) &= |U_0 + U_1(x, y)|^2 \\ &= |U_0|^2 + |U_1(x, y)|^2 + U_0 \cdot U_1^*(x, y) + U_0^* \cdot U_1(x, y) \end{aligned}$$

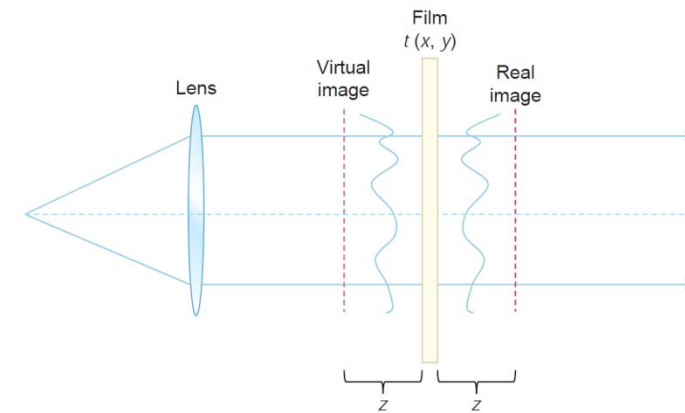


# In-line Holography

- Reading the hologram essentially means illuminating it as if it is a new object (Fig. 6.2). The field scattered from the hologram is the product between the illuminating plane wave (assumed to be ) and the transmission function

$$t(x, y) = a + bI(x, y)$$

$$\begin{aligned} U(x, y) &= U_0 \cdot t(x, y) \\ &= U_0 \left( a + b|U_0|^2 \right) + bU_0 \cdot |U_1(x, y)|^2 \\ &\quad + b|U_0|^2 \cdot U_1(x, y) + b|U_0|^2 \cdot U_1^*(x, y) \end{aligned}$$



- The last two terms contain the scattered complex field and its back-scattered counterpart. The observer behind the hologram is able to see the image that resembles the object.
- The backscattering field forms a virtual image that overlaps with the focused image.

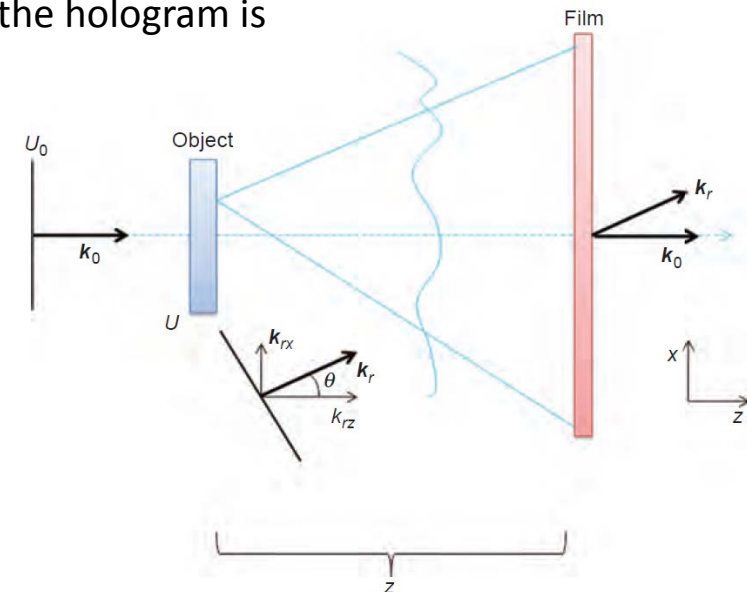
# Off-Axis Holography

- Emmitt Leith and Juris Upatnieks developed this off-axis reference hologram, the evolution from Gabor's inline hologram.
- Writing the hologram:
  - The field distribution across the film, i.e. the Fresnel diffraction pattern is a convolution between the transmission function of the object  $U$ , and the Fresnel kernel

$$U_F(x, y) = U(x, y) \circledast e^{\frac{ik_0(x^2+y^2)}{2z}}$$

- The resulting transmission function associated with the hologram is proportional to the intensity, i.e.

$$t(x, y) = |U_F(x, y)|^2 + |U_r|^2 + U_F(x, y) \cdot |U_r| \cdot e^{-ik_{rx} \cdot x} + U_F^*(x, y) \cdot |U_r| \cdot e^{ik_{rx} \cdot x}$$

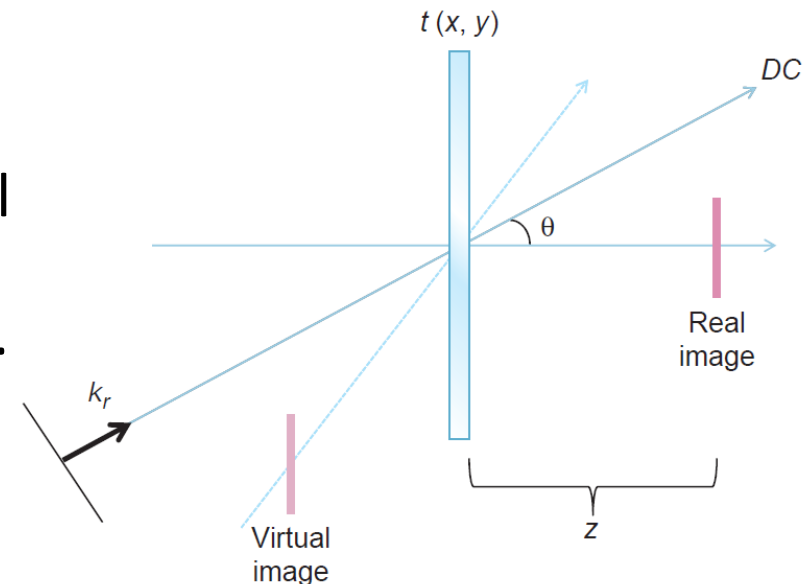


# Off-Axis Holography

- Reading the hologram:
  - Illuminating the hologram with a reference plane wave,  $U_r$ , the field at the plane of the film becomes

$$\begin{aligned}U_h(x, y) &= |U_r| \cdot e^{ik_r \cdot r} \cdot t(x, y) \\&= |U_F(x, y)|^2 \cdot |U_r| \cdot e^{ik_r \cdot r} + |U_r|^3 \cdot e^{ik_r \cdot r} \\&\quad + U_F(x, y) \cdot |U_r|^2 + U_F^*(x, y) \cdot |U_r|^2 \cdot e^{i2k_{rx} \cdot x}\end{aligned}$$

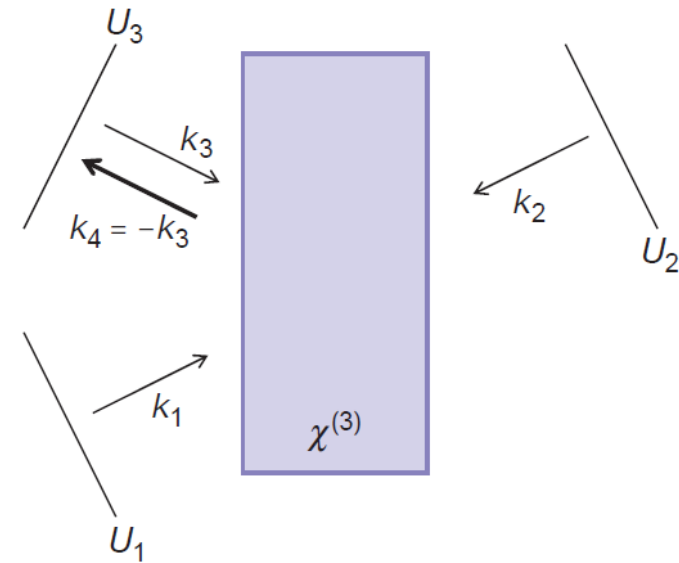
- The last two terms recover the Real image and the virtual image at an angle different than the real image.



# Nonlinear (Real Time) Holography or Phase Conjugation

- Nonlinear *four-wave mixing* can be interpreted as *real-time holography*
- The idea relies on third-order nonlinearity response of the material used as writing/reading medium .
- Two strong field  $U_1$ ,  $U_2$ , that are time reverse of each other and incident on the  $\chi^{(3)}$ . An object field  $U_3$  is applied simultaneously, inducing the nonlinear polarization

$$\begin{aligned}
 P^{(NL)}(-\omega_4 = \omega_1 + \omega_2 - \omega_3) &= \frac{1}{2} \chi^{(3)} U_1 U_2 U_3^* e^{i[\omega_3 t - (k_1 - k_1 + k_3)r]} \\
 &= \frac{1}{2} \chi^{(3)} |U_1|^2 \cdot U_3^* \cdot e^{-i\omega_4 t + i k_4 \cdot r}
 \end{aligned}$$



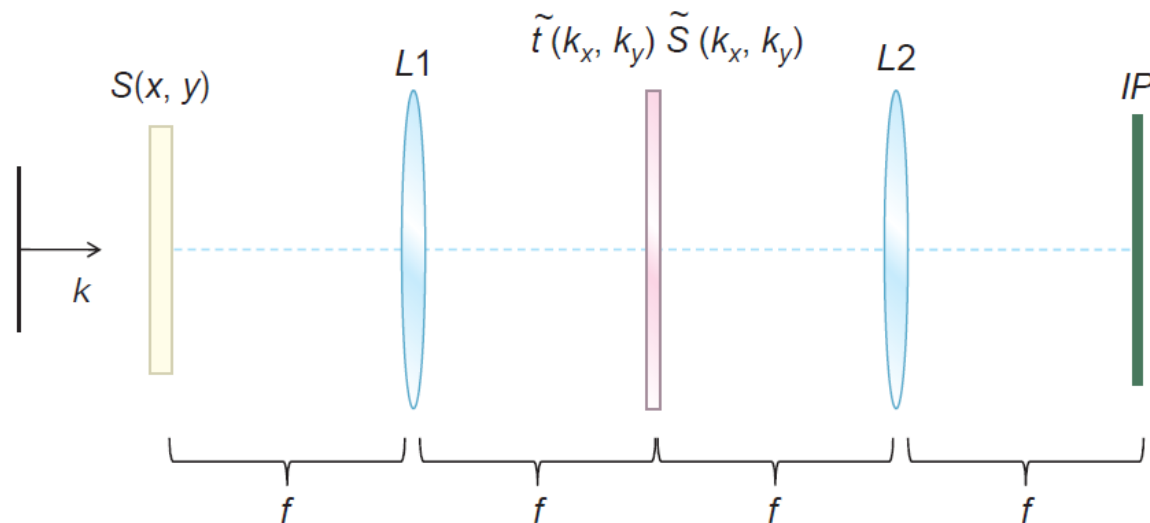
Clearly, the field emerging from the material,  $U_4$ , is the time-reversed version of  $U_3$ , i.e.  $\omega_4 = -\omega_3$  and  $\mathbf{k}_4 = -\mathbf{k}_3$ , as indicated by the complex conjugation ( $U_3^*$ ).

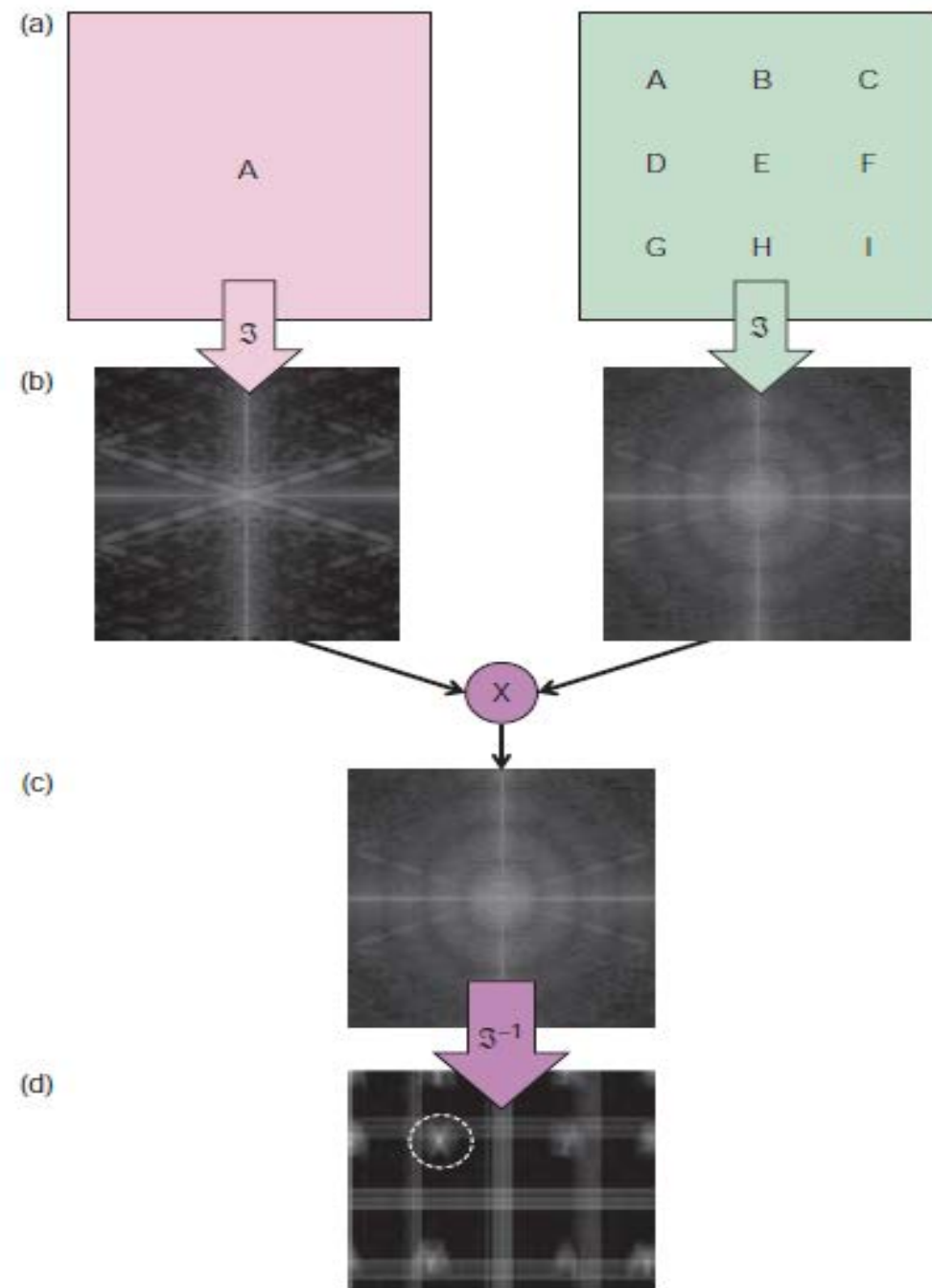
# Digital Hologram

## *writing*

- idea is to calculate the cross-correlation between the known signal of interest and an unknown signal which, as a result, determines (i.e., recognizes) the presence of the first in the second
- The result field on the image plane is characterized by the cross correlation between the image in interest and the image being compared

$$U(x, y) = t_0 S(x, y) + S(x, y) \otimes t_1(x - x_0, y)$$

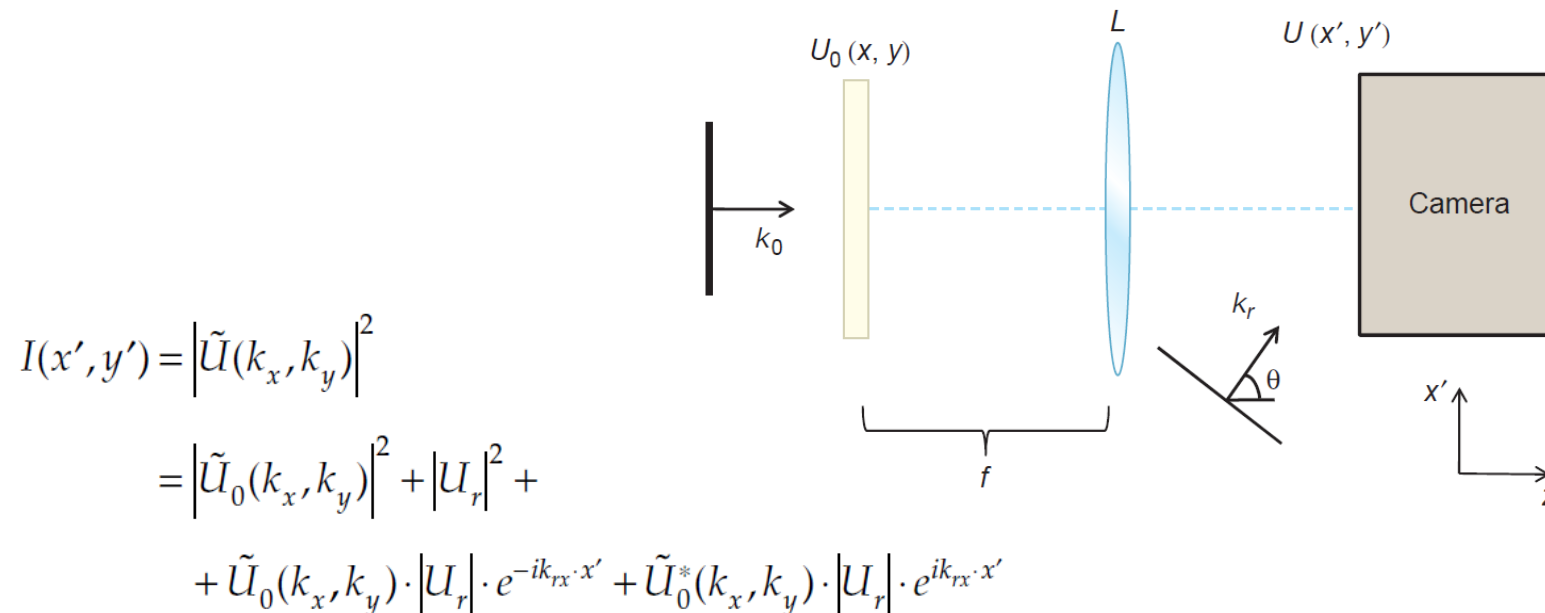




# Digital Holography

## *reading*

- The transparency containing the signal of interest is illuminating by a plane wave. The emerging field,  $U_0$ , is Fourier transformed by the lens at its back focal plane, where the 2D detector array is positioned. The off-axis reference field  $U_r$  is incident on the detector at an angle  $\theta$ .
- Fourier Transforms are numerically processed with FFT algorithm





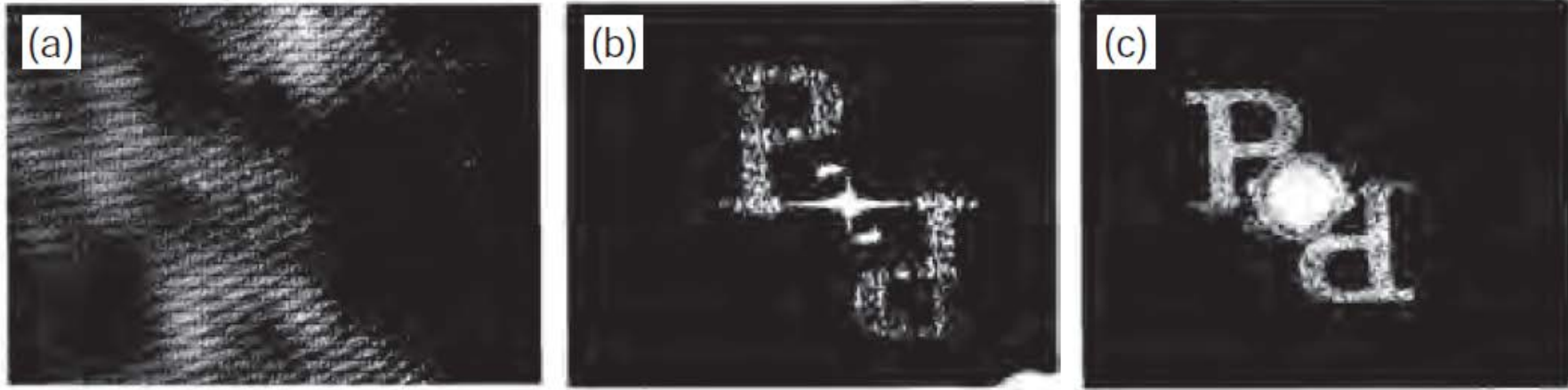


**FIGURE 6.9** (a) Hologram stored in computer memory; (b) display of the image reconstructed by digital computation; (c) image obtained optically from a photographic hologram, shown for comparison. (Reprinted with permission from J. W. Goodman and R. W. Lawrence, *Appl. Phys. Lett.* 11, 77 (1967). Copyright 1967, American Institute of Physics.)

# Chap. 8

Principles of Full-Field QPI

# Interferometric Imaging

- The image field can be expressed in space-time as

$$U_i(x, y; t) = |U_i(x, y)| \cdot e^{-i[\langle \omega \rangle t - \langle \mathbf{k} \rangle \cdot \mathbf{r} + \phi(x, y)]}$$

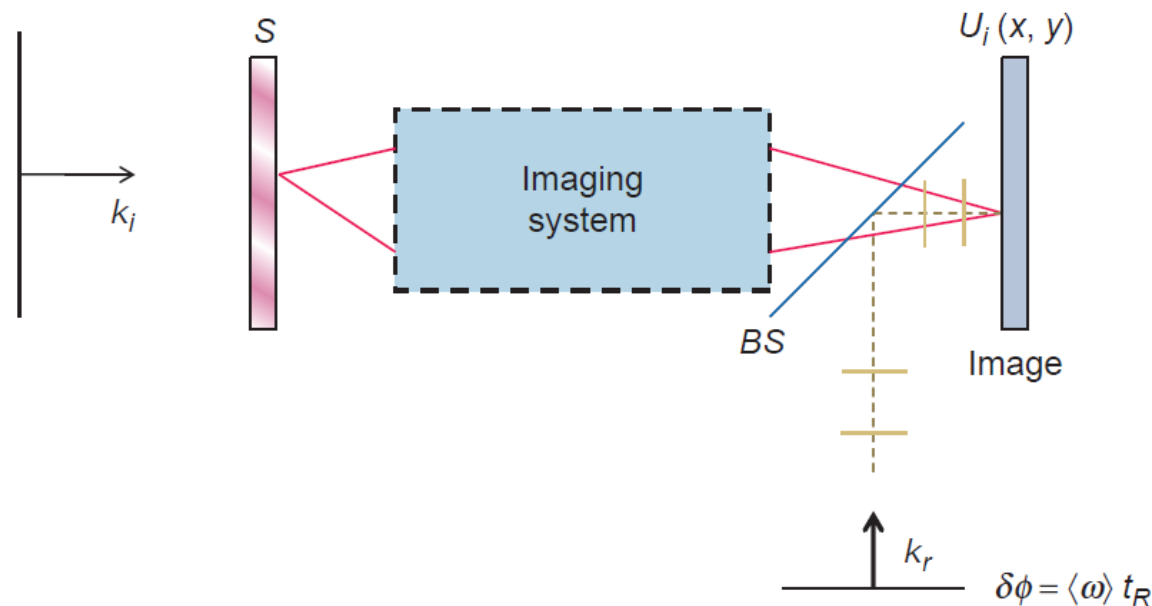
- Detector is only sensitive to intensity, phase information is lost in the modulus square of field.  $|U(x, y, t)|^2$
- Mixing with a reference field  $U_r$

$$I(x, y) = |U_i(x, y)|^2 + |U_R|^2 + 2|U_R| \cdot |U_i(x, y)| \\ \cdot \cos \left[ \langle \omega \rangle (t - t_R) - (\langle \mathbf{k} \rangle - \mathbf{k}_R) \cdot \mathbf{r} + \phi(x, y) \right]$$

# Temporal Phase Modulation: Phase-Shifting Interferometry

- The idea is to introduce a control over the phase difference between two interfering fields, such that the intensity of the resulting signal has the form

$$I(\delta\phi) = I_1 + I_2 + 2\sqrt{I_1 I_2} \cdot \cos[\phi + \delta\phi]$$



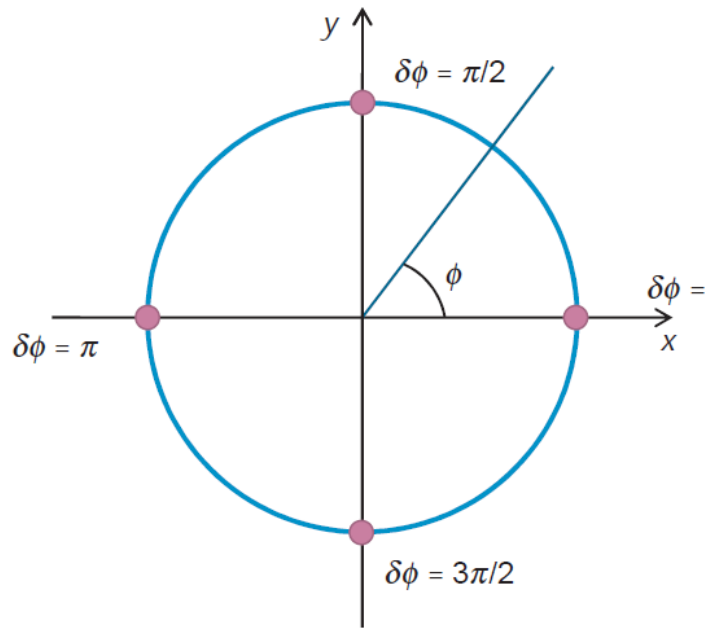
# Temporal Phase Modulation: Phase-Shifting Interferometry

- Three unknown variables:  $I_1$  ,  $I_2$  and the phase difference  $\phi$
- Minimum three measurements is needed
- However, three measurements only provide  $\phi$  over half of the trigonometric circle, since sine and cosine are only **bijective** over half circle, i.e.  $(-\frac{\pi}{2}, \frac{\pi}{2})$  and  $(0, \pi)$  respectively
- Four measurements with phase shift in  $\frac{\pi}{2}$  increment.

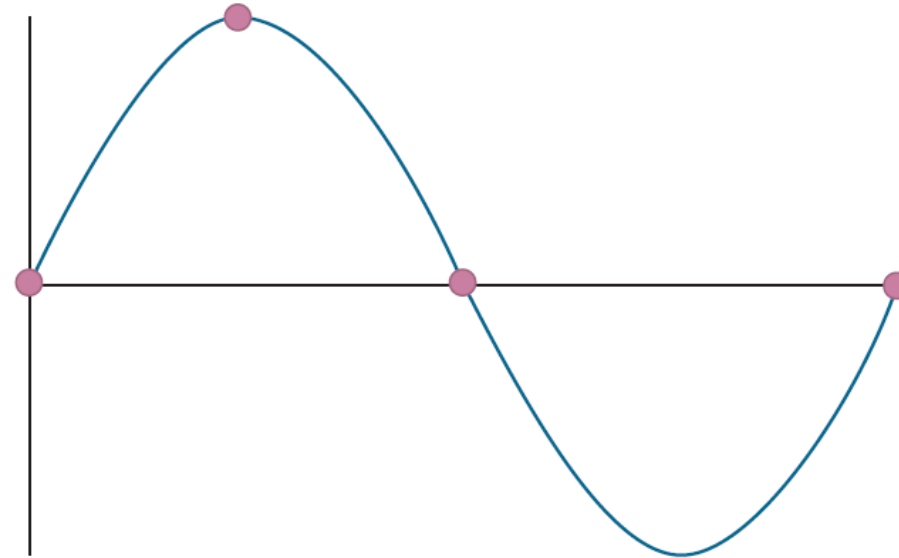
$$\phi = \arg \left[ I(0) - I(\pi), I\left(\frac{3\pi}{2}\right) - I\left(\frac{\pi}{2}\right) \right]$$

# Temporal Phase Modulation: Phase-Shifting Interferometry

(a)



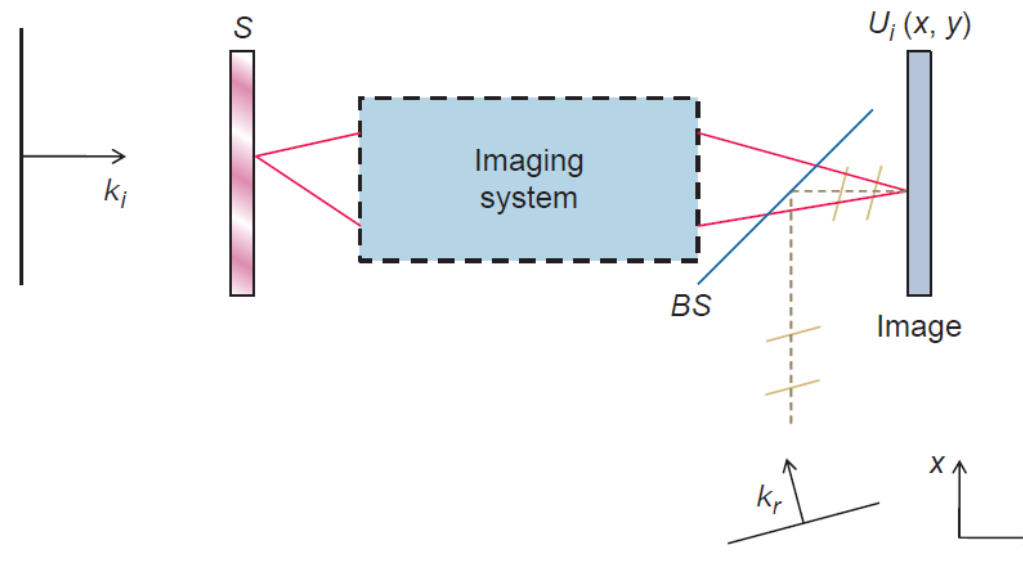
(b)



# Spatial Phase Modulation: Off-Axis Interferometry

- Off-axis interferometry takes advantage of the ***spatial phase modulation*** introduced by the *angularly shifted* reference plane wave

$$I(x, y) = |U_i(x, y)|^2 + |U_r|^2 + 2|U_r| \cdot |U_i(x, y)| \cdot \cos[\Delta k \cdot x + \phi(x, y)]$$



# Spatial Phase Modulation: Off-Axis Interferometry

- The goal is to isolate  $\cos[\Delta k x' + \phi(x', y)]$  and calculate the imaginary counterpart through a Hilbert Transform

$$\sin[\Delta k \cdot x + \phi(x, y)] = P \int \frac{\cos[\Delta k \cdot x' + \phi(x', y)]}{x - x'} dx'$$

- Finally the argument is obtained uniquely as

$$\phi(x, y) + \Delta k x = \arg[\cos(\Delta k x + \phi), \sin(\Delta k x + \phi)]$$

- the frequency of modulation,  $\Delta k$ , sets an upper limit on the highest spatial frequency resolvable in an image.



# Phase Unwrapping

- Phase measurements yields value within  $(-\pi, \pi]$  interval and modulo( $2\pi$ ). In other words, the phase measurements cannot distinguish between  $\phi_0$ , and  $\phi_0 + \frac{\pi}{2}$
- Unwrapping operation searches for  $2\pi$  jumps in the signal and corrects them by adding  $2\pi$  back to the signal.

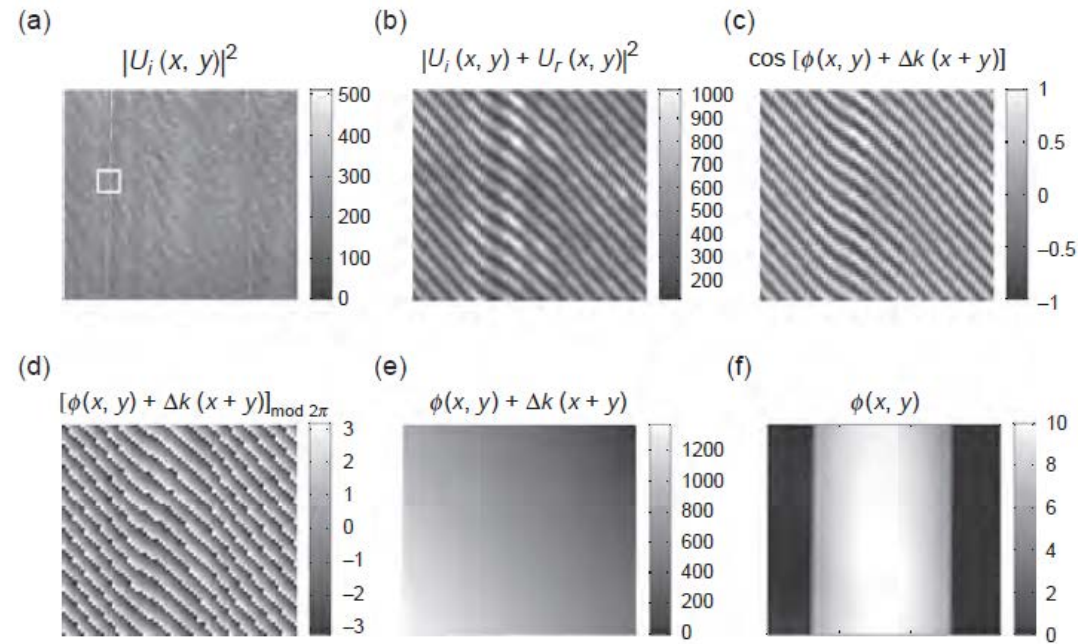
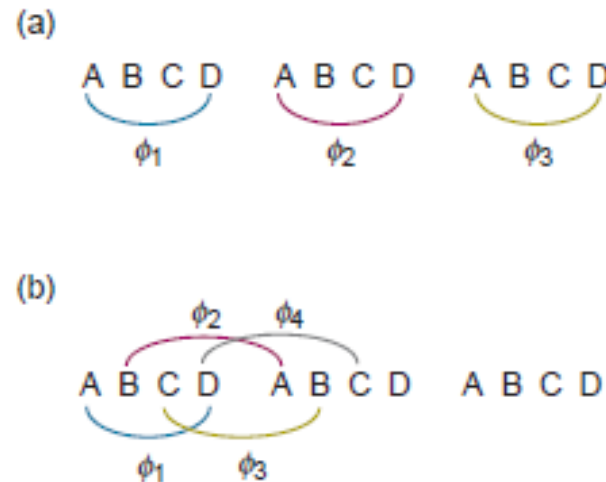


**FIGURE 8.6** (a) Transmission intensity image of a transparent object (optical fiber); (b), (c), (d) interferogram, sinusoidal signal, and wrapped phase, respectively, measured from the white box indicated in (a); (e) full-field unwrapped phase, (f) full-field quantitative phase image. [Reproduced with permission from T. Ikeda, G. Popescu, R. R. Dasari and M. S. Feld, Hilbert phase microscopy for investigating fast dynamics in transparent systems, *Opt. Lett.*, 30, 1165–1168 (2005). Copyright Optical Society of America 2005.]

# Figures of Merit in QPI

- **Temporal Sampling: Acquisition Rate**

- Must be at least twice the frequency of the signal of interest, according to Nyquist sampling theorem.
- In QPI acquisition rate vary from application: from  $>100\text{Hz}$  in the case of membrane fluctuations to  $<1\text{mHz}$  when studying the cell cycle.
- Trade-off between acquisition rate and sensitivity.
- Off-axis has the advantage of “single shot” over phase-shifting techniques, which acquires at best four time slower than that of the camera.



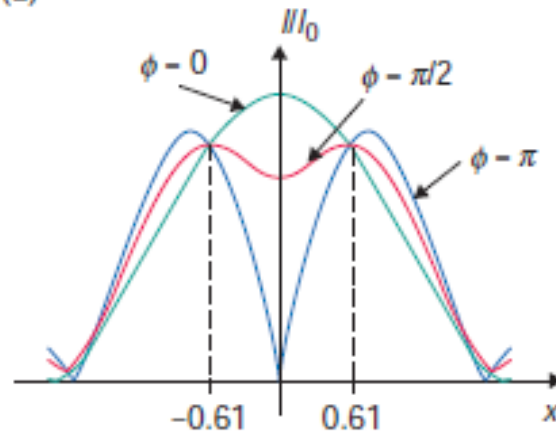
# Figures of Merit in QPI

- **Spatial Sampling: Transverse Resolution**

- QPI offer new opportunities in terms of transverse resolution, not clear-cut in the case of coherent imaging.
- The phase difference between the two points has a significant effect on the intensity distribution and resolution.
- Phase shifting methods are more likely than phase shifting method to preserve the diffraction limited resolution

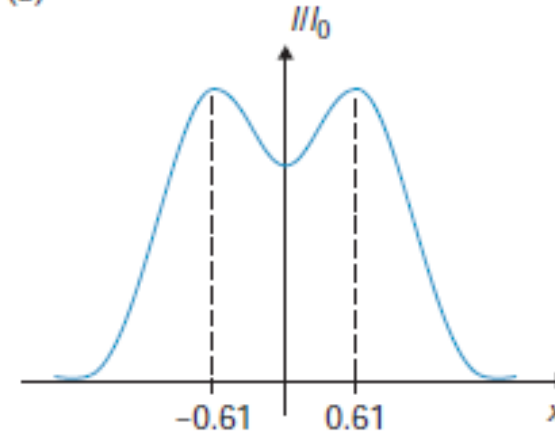
$$I(x) = \left| \frac{J_1[\pi(x-0.61)]}{\pi(x-0.61)} + e^{i\phi} \frac{J_1[\pi(x+0.61)]}{\pi(x+0.61)} \right|^2$$

(a)



$$I_{incoherent}(x) = \left\{ \frac{J_1[\pi(x-0.61)]}{\pi(x-0.61)} \right\}^2 + \left\{ \frac{J_1[\pi(x+0.61)]}{\pi(x+0.61)} \right\}^2$$

(b)



# Figures of Merit in QPI

- **Temporal Stability: Temporal-Phase Sensitivity**

- Assess phase stability experimentally: perform successive measurements of a stable sample and describe the phase fluctuation of one point by its standard deviation

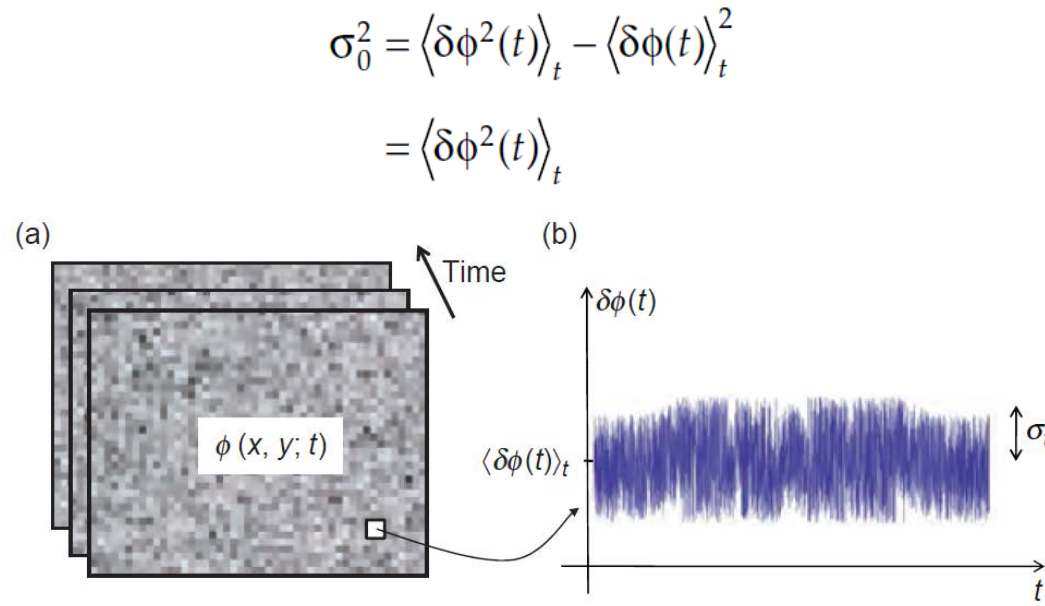


**FIGURE 8.9** (a) Time-series of quantitative phase images. (b) Phase noise at the point shown in (a). The average and standard deviation are indicated.

# Figures of Merit in QPI

- **Temporal Stability: Temporal-Phase Sensitivity**

- Reducing Noise Level:**

- Simple yet effective means is to reference the phase image to a point in the field of view that is known to be stable. This reduces the common mode noise, i.e. phase fluctuations that are common to the entire field of view.

$$\phi'(x, y, t) = \phi(x, y, t) - \phi(x_0, y_0, t)$$

- A fuller descriptor of the temporal phase noise is obtained by computing numerically the power spectrum of the measured signal. The area of the normalized spectrum gives the variance of the signal

$$\begin{aligned}\sigma_0^2 &= \sum_i \Phi(\omega_i) \Delta\omega \\ &= \sum_i \sigma_i^2\end{aligned}$$

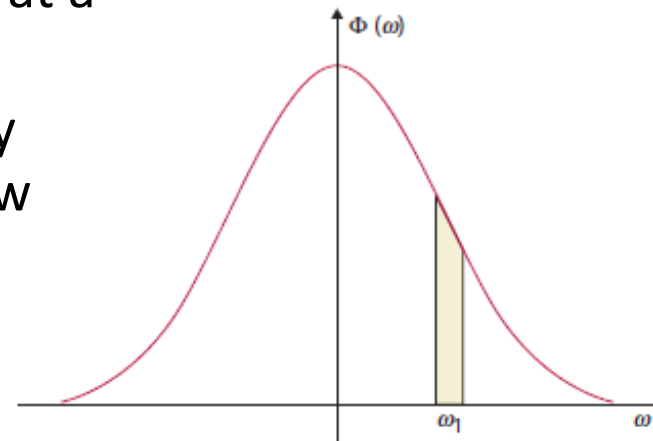
# Figures of Merit in QPI

- **Temporal Stability: Temporal-Phase Sensitivity**

- Reducing Noise Level:**

- Function  $\Phi$  is the analog of the **noise equivalent power (NEP)** commonly used as a figure of merit for photodetectors.
  - **NEP** represents the smallest phase change (in rad) that can be measured (SNR =1) at a frequency bandwidth of 1 rad/s.
  - High sensitivity thus can be achieved by locking the measurement onto a narrow band of frequency.

$$\begin{aligned}\sigma_0^2 &= \sum_i \Phi(\omega_i) \Delta\omega \\ &= \sum_i \sigma_i^2\end{aligned}$$



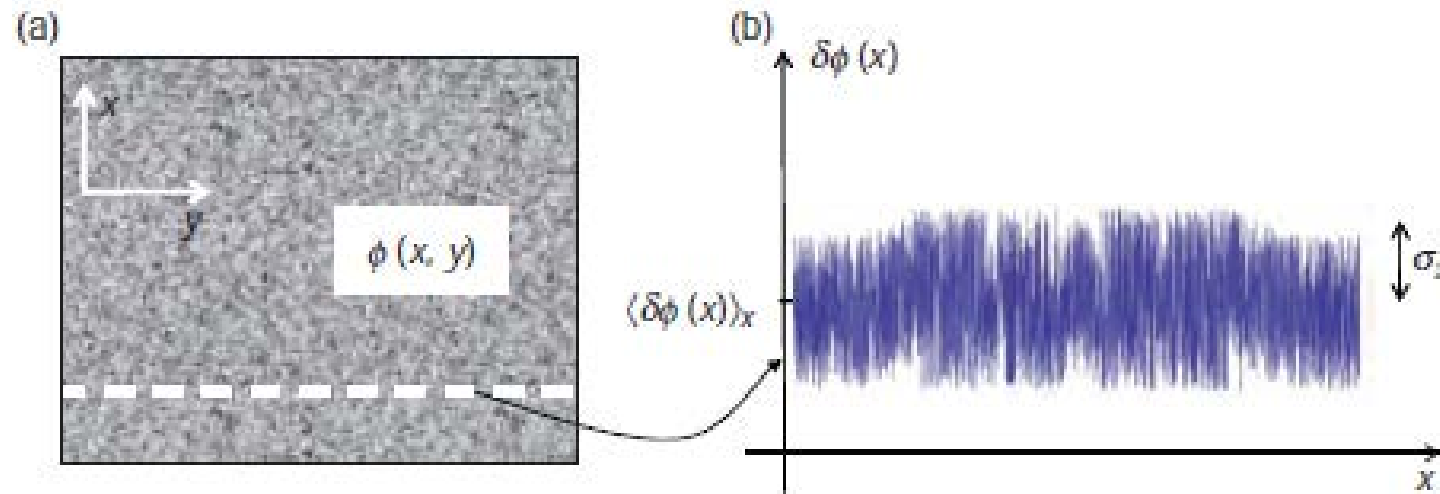
# Figures of Merit in QPI

- **Temporal Stability: Temporal-Phase Sensitivity**
  - Passive stabilization
  - Active stabilization
  - Differential measurements
  - Common path interferometry

# Figures of Merit in QPI

- **Spatial Uniformity: Spatial Phase Sensitivity**

- Analog to the “frame-to-frame” phase noise, there is a “point-to-point” (spatial) phase noise affects measurements.





# Figures of Merit in QPI

- **Spatial Uniformity: Spatial Phase Sensitivity**

- The standard deviation for the entire field of view, following the time domain definition:

$$\sigma_r = \sqrt{\left\langle \left[ \delta\phi(x, y) - \langle \delta\phi(x, y) \rangle_{x,y} \right]^2 \right\rangle_{x,y}}$$

- The normalized spectrum density

$$\Phi(k_x, k_y) \propto \left| \int_A \delta\phi(x, y) \cdot e^{i(k_x \cdot x + k_y \cdot y)} dx dy \right|^2$$

- Thus variance defined as

$$\int_{A_k} \Phi(k_x, k_y) dk_x dk_y = \sigma_0^2$$

# Figures of Merit in QPI

- **Spatial Uniformity: Spatial Phase Sensitivity**

- Again, phase sensitivity can be increased significantly if the measurement is band-passed around a certain spatial frequency

- **Spatial and Temporal power spectrum**

$$\Phi(\mathbf{k}, \omega) \propto \left| \int \int \int_{-\infty}^{\infty} \delta\phi(\mathbf{r}, t) \cdot e^{i(\omega t - \mathbf{k} \cdot \mathbf{r})} dt d^2\mathbf{r} \right|^2$$

# Summary of QPI Approaches and Figures of Merit

- There is no technique that performs optimally with respect to all figures of merit identified

	Acquisition rate	Transverse resolution	Temporal sensitivity	Spatial sensitivity
Off-axis	X			
Phase-shifting		X		
Common-path			X	
White light				X

# Summary of QPI Approaches and Figures of Merit

- Thus, there are  $C_4^2 = 6$  possible combinations of two methods, as follows
  - Off-axis and phase-shifting (discussed in Sec. 9.1.2)
  - Phase shifting and white light (Sec. 10.1)
  - Phase shifting and common path (Sec. 11.1.)
  - Off-axis and common path (Sec. 11.2)
  - Common path and white light (Chap. 12)
  - Off-axis and white light (Sec. 14.2.2., this method is also common path)

# Summary of QPI Approaches and Figures of Merit

- Thus, there are  $C_4^3 = 4$  possible combinations of three methods, as follows
  - Phase shifting, common path, white light (Chap. 12)
  - Off-axis, common path, white light (Sec. 14.2.2.)
  - Off-axis, phase shifting, common path (see, for instance, Refs. 15 and 16)
  - Off-axis, phase shifting, white light (perhaps to be developed)